AROMATIC NYLONS FOR TRANSPARENT ARMOR APPLICATIONS

John W. Song[1*], Joel Lofgren[1], Kyle D. Hart[1], Nick Tsantinis[1], Roy Paulson[2] and Jay N. Hatfield[3]
1: U.S. Army Research, Development and Engineering Command, Soldier Systems Center, Natick Soldier Center, AMSRD-NSC-IP-B, Natick, MA 01760-5019
2: Paulson Manufacturing Corp., Temecula, CA 92592-5984
3: Degussa Corporation, High Performance Polymers, Parsippany, NJ 07054-0677

ABSTRACT

Failure and kinetic energy absorption mechanisms upon ballistic impact of two new types of nylons, TROGAMID T-5000 (T-5000) and TROGAMID-CX7323 (CX-7323) as well as traditional materials such as polycarbonate (PC) and polymethylmethacrylate (PMMA) were examined and compared. Under ballistic impact, T-5000 showed brittle failure similar to PMMA, while CX-7323 exhibited ductile behavior similar to PC. Like PC and PMMA, the failure modes of T-5000 and CX-7323 are different from each other. However, unlike PC and PMMA, the overall ballistic performance of these two TROGAMIDs were similar to each other. Among these four materials, PMMA exhibited the most sensitive response to frequency or impact velocity by showing the most rapid increase of kinetic energy absorption with increasing impact velocity or sample thickness. For monolithic samples the ballistic impact resistance of these two TROGAMIDs is noticeably better than PC and PMMA for a wide range of thicknesses. Furthermore, the hybrid of these two materials shows a synergistic effect, which is similar to behavior observed in hybrids of PC and PMMA. The data obtained from flat plaques indicate that the improvement of ballistic resistance of these new nylon materials from the currently fielded system could be significant in certain applications.

1. INTRODUCTION

PC and PMMA are commonly used materials for current transparent armor applications. Our earlier studies showed that the distinct difference in failure behavior of these two materials is one of the major responsible parameters of the kinetic energy absorption capabilities of these materials [1, 2]. Song and Hsieh [1] found that PMMA is sensitive to impact velocity. At a given thickness, as the velocity increases, the failure mode changes from brittle cut-off at low velocity to the localized severe micro-crack at high velocity. The former mode produces no or minimal energy absorption. However, the latter mode, which shows kinetic energy absorption through localized micro cracking around the impact area, clearly showed enhanced energy absorption. These results were verified by changing the thickness of the evaluated samples. PC, which exhibits ductile behavior with no stress whitening, shows significantly higher energy absorption than PMMA for thin samples and levels off as the thickness reaches certain levels. However, as increasing the thickness, the kinetic energy absorption rate of PMMA upon ballistic impact was much greater than PC. With these unique characteristics, monolithic PMMA starts to outperform monolithic PC at around 10mm thickness or 3 lbs/ft^2 areal density.

TROGAMID® T-5000 and TROGAMID® CX-7323 are permanently transparent, high strength and excellent chemically resistant materials produced by Degussa High Performance Polymers. Figure 1 shows the chemical structures of TROGAMID T-5000 and TROGAMID CX-7323 as well as PC and PMMA. The potential for ballistic impact application of TROGAMID® T grade was recognized during the early 1970's when this material was first introduced [3, 4] but was not fully exploited in the past. As shown in Figure 1, T-5000 contains partially aromatic units that impart rigidity and high heat resistance. CX-7323 incorporates the long aliphatic segment in the structure. CX-7323 is a microcrystalline material that is permanently transparent. The crystal size is too small to scatter visible light and the degree of crystallinity is negligible.

This work examines the various properties as well as ballistic impact behavior of two grades of TROGAMID® (T-5000 and CX-7323). The obtained data will be correlated and compared with PC and PMMA. Hybrid systems of these materials will also be discussed.

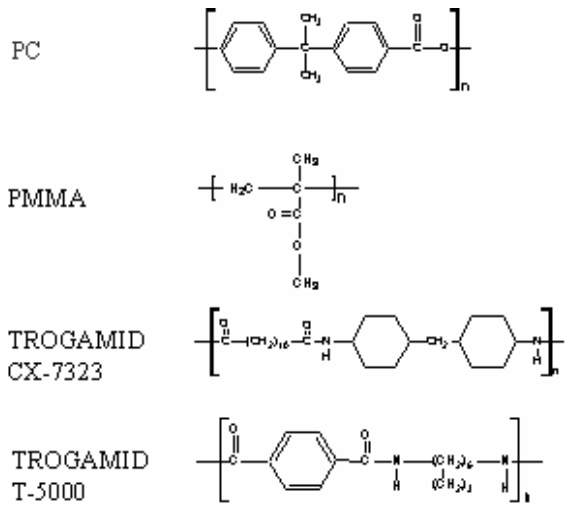

Figure 1. Materials used in this study.

Report Documentation Page

Form Approved
OMB No. 0704-0188

Public reporting burden for the collection of information is estimated to average 1 hour per response, including the time for reviewing instructions, searching existing data sources, gathering and maintaining the data needed, and completing and reviewing the collection of information. Send comments regarding this burden estimate or any other aspect of this collection of information, including suggestions for reducing this burden, to Washington Headquarters Services, Directorate for Information Operations and Reports, 1215 Jefferson Davis Highway, Suite 1204, Arlington VA 22202-4302. Respondents should be aware that notwithstanding any other provision of law, no person shall be subject to a penalty for failing to comply with a collection of information if it does not display a currently valid OMB control number.

1. REPORT DATE	2. REPORT TYPE	3. DATES COVERED
01 NOV 2006	**N/A**	**-**

4. TITLE AND SUBTITLE	5a. CONTRACT NUMBER
Aromatic Nylons For Transparent Armor Applications	5b. GRANT NUMBER
	5c. PROGRAM ELEMENT NUMBER
6. AUTHOR(S)	5d. PROJECT NUMBER
	5e. TASK NUMBER
	5f. WORK UNIT NUMBER
7. PERFORMING ORGANIZATION NAME(S) AND ADDRESS(ES) **U.S. Army Research, Development and Engineering Command, Soldier Systems Center, Natick Soldier Center, AMSRD-NSC-IP-B, Natick, MA 01760-5019**	8. PERFORMING ORGANIZATION REPORT NUMBER
9. SPONSORING/MONITORING AGENCY NAME(S) AND ADDRESS(ES)	10. SPONSOR/MONITOR'S ACRONYM(S)
	11. SPONSOR/MONITOR'S REPORT NUMBER(S)

12. DISTRIBUTION/AVAILABILITY STATEMENT
Approved for public release, distribution unlimited

13. SUPPLEMENTARY NOTES
See also ADM002075., The original document contains color images.

14. ABSTRACT

15. SUBJECT TERMS

16. SECURITY CLASSIFICATION OF:			17. LIMITATION OF ABSTRACT	18. NUMBER OF PAGES	19a. NAME OF RESPONSIBLE PERSON
a. REPORT	b. ABSTRACT	c. THIS PAGE			
unclassified	**unclassified**	**unclassified**	**UU**	**8**	

Standard Form 298 (Rev. 8-98)
Prescribed by ANSI Std Z39-18

2. EXPERIMENTAL

2.1 Materials

Injection molded TROGAMID® T-5000 and TROGAMID® CX-7323 plaques of various thicknesses ranging from 1mm 10mm were obtained from Degussa Corporation, NJ and Paulson Manufacturing Corporation, CA. Monolithic PC, Lexan™, and PMMA, Plexiglas G™ of various thicknesses ranging from 1.59mm to 25.4mm were also purchased from General Electric and AtoHaas Company, respectively.

2.2 Thermal Analysis

Differential Scanning Calorimetry (DSC) and Dynamic Mechanical Analysis (DMA) were conducted to evaluate the materials response as a function of temperature.

2.2.1 Differential Scanning Calorimetry (DSC)

DSC evaluation was performed using TA Instrument DSC Q100. Aluminum hermatic pans were used to hold the samples. Samples were prepared by cutting small pieces of polymer pellets and small pieces from the flat plaque. Indium was used as a temperature calibration. Samples were heated at a rate of 10°C/min.

2.2.2 Dynamic Mechanical Analysis (DMA)

DMA evaluation was performed using TA Instruments DMA Q800. For general observation of viscoelastic behavior of the materials over the broad range of temperatures, single cantilever mode was used. In all cases, the heating rate used was 2°C/min. Three-point bending mode was also used to observe the bending behavior of the materials at the broad range of frequencies at 30°C. Samples used were rectangular in shape in both cases.

2.3 Hardness Testing

ASTM D-2240-02b hardness testing was performed using a Model 1700 Type-D Rex durometer with a 10kg weight over the axis of the indentor.

2.4 Three Point Bending Evaluation

Three point bending properties were obtained using the Instron 5500R. Sample dimensions and the test conditions such as span distance and crosshead speed were determined by closely following ASTM D790. DMA 3-point bending mode, through frequency sweep at 30°C, was also used to observe the bending behavior over the broad range of frequencies and to compare with the Instron test results.

2.5 Compression Property Evaluation

Quasi-static compression testing was performed using an Instron 5500. To simulate 0.22 caliber Fragment Simulating Projectile (FSP), commonly used in ballistic evaluations, the fragment was mounted at the tip of the indentor. Samples were placed between two one-inch aluminum plates with 3" diameter aperture. The two plates were then bolted together using 16 ft-lbf of torque, and the adjoined plates were positioned on the Instron. A 10kN load cell was used for the testing. Testing was performed at a compression rate of 10mm/min. In the case of PC and PMMA, the effect of compression speed was also evaluated using four different rates between 1 and 50mm/min.

2.6 Abrasion Resistance

Taber as well as sand blast abrasion resistance were measured using a Taber 5130 Abraser and in-house apparatus, respectively. For the taber abrasion test, CS-10F abrasion test wheels were used with 500g weight.
Sand used for sand blast testing was silica sand from US silica with grain size of 300 – 350μm. Approximately 2" x 2.5" samples were placed in 12" x 12" wind tunnel. The distance between the output port of sand and the sample was approximately one yard. The wind speed was approximately 16m/sec and the mass flow rate of the sand was 212.25g/min. Two samples were tested at the same time.

Abrasion resistance was determined by the changes in percent haze before and after exposure to the abraders (Taber abrasion wheel or Sand). Percent haze was measured using a Hazemeter UX-10 from Gardner Laboratory.

2.7 Ballistic Evaluations

Ballistic evaluations of the materials were conducted for monolithic as well as hybrid systems of these materials. Samples measuring approximately 4" x 4" were mounted between two aluminum plates with four 2" diameter circular openings on the four corners of the plate. This sample holder was then clamped in the center of the high-velocity impact test apparatus. The projectile used for all testing was a 17-grain (1.1 gram weight), .22 caliber (0.22 inch diameter) fragment simulating projectile (FSP). Assuming the mass (M) of the projectile is constant during the penetration of the target, kinetic energy absorption (KE) by samples was calculated as following.

$$KE = 1/2M(V_s^2 - V_r^2) \quad (1)$$

where V_s and V_r are the striking and residual velocities, respectively.

3. RESULTS AND DISCUSSIONS

3.1 DSC Analysis

Figure 2 and Table 1 show the results of the DSC evaluation on these materials. In all cases, a heating rate of 10°C/min was used. The glass transition temperatures of PC and T-5000 were close to each other at around 150°C followed by CX-7323 and PMMA. However, microcrystalline CX-7323 exhibited cold crystallization (T_c) immediately after the T_g, starting around 150°C and peaking at 165°C. The melting temperature (T_m) was observed between 230°C and 260°C. Table 1 also shows the T_g of these materials obtained from the E" peak of DMA scans observed at 0.05hz frequency and they agree well.

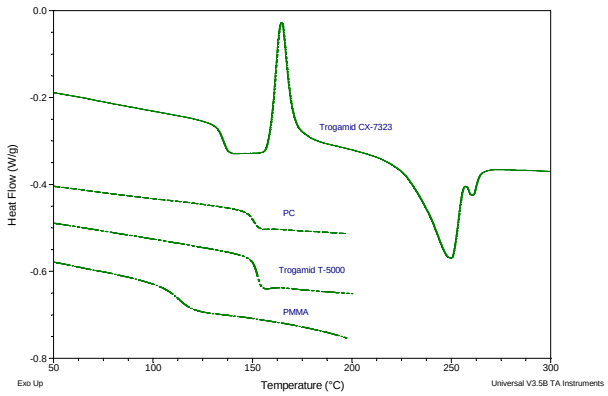

Figure 2. DSC thermogram of PC, PMMA, T-5000 and CX-7323.

Table 1. Thermal properties of polymers. T_g, T_c and T_m are glass transiton, crystalline and melting temperatures, respectively. H_c and H_m are heat of crystallization and heat of melting, respectively

Samples	T_g (°C)		T_c (°C)	H_c (J/g)	T_m (°C)	H_m (J/g)
	DSC	DMA*				
PC	150.46	153.16	NA	NA	NA	NA
PMMA	113.31	122.10	NA	NA	NA	NA
T-5000	152.28	150.51	NA	NA	NA	NA
CX-7323	135.06	137.10	158.48	18.71	228.78	26.48

*: T_g obtained from E" peak values of DMA analysis

3.2 DMA Analysis

Figure 3 is the dynamic mechanical behavior observed using the single cantilever mode. As shown in Figure 3, PMMA and T-5000 exhibit higher flexural modulus values below T_g than the other two materials. Polycarbonate and CX-7323 showed lower flexural modulus below the T_g region than PMMA and T-5000. The increasing modulus at around 150°C of CX-7323 is due to the cold crystallization, which was observed in the DSC scan (see Figure 2). The glass transition temperatures (T_g) obtained from E" of these materials are listed in Table 1.

3.3 Hardness Testing

Table 2 summarizes the hardness of these materials. As can be seen, PMMA exhibits slightly higher hardness than the others, which is expected from the DMA results. PC and T-5000 performed similarly and CX-7323 was the softest among them.

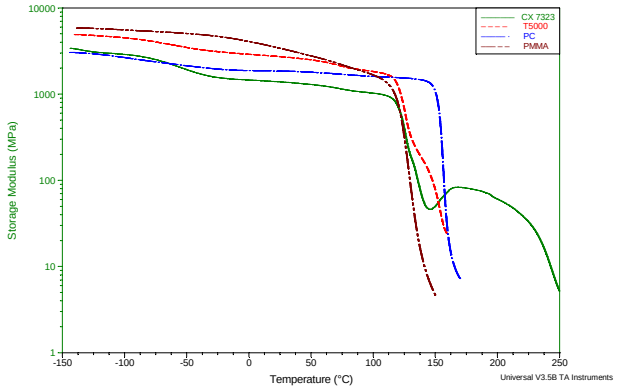

Figure 3. DMA scan of Flexural modulus (E') as a function of temperature of PC, PMMA T-5000 and CX-7323

Table 2. Hardness data.

Materials	Thickness (mm)	Hardness (Shore D)	Std. Dev
PMMA	9.22	90.42	0.66
PC	5.84	84.13	0.44
T-5000	9.96	83.88	0.38
CX-7323	9.97	80.42	0.97

3.4 Three Point Bending Evaluation

Three point bending evaluations were performed with an Instron 5500R as well as the frequency sweep of DMA evaluations at room temperature (30°C). Table 3 shows the bending modulus values obtained from the Instron and DMA. To closely imitate the instron test conditions, the lowest frequency (0.05Hz) value from the DMA was chosen for the comparison. The values obtained from the Instron and lowest frequency DMA data agree well with each other except in the case of PMMA where the DMA values are noticeably higher than Instron values. As shown in Figure 4, it is interesting to note that the flexural storage modulus of PMMA

increased exponentially with frequency. This suggests that at higher frequencies, the modulus of PMMA could be significantly greater than that of the other three materials. In the earlier studies on ballistic resistance of PMMA and PC, PMMA exhibited higher energy absorption capability than PC upon high velocity impact. This result indicates that the increased modulus at higher frequency contributed to increased kinetic energy absorption upon ballistic impact. Yield stress, yield strain and the toughness at the yield points obtained from the Instron are also listed in Table 3.

Table 3. 3-point bending properties of PC, PMMA T-5000 and CX-7323.

Materials	Flexural Modulus (Mpa)	Flexural Modulus (Mpa) DMA at 0.05hz	Yield Stress (Mpa)	Yield Strain (mm/mm)	Yield Toughness (Mpa)
PMMA	2450	3363	102.6	0.0786	5.38
PC	2200	2199	92.6	0.0688	4.36
T-5000	3140	3111	113.3	0.0725	5.86
CX-7323	1566	1552	74.2	0.0739	3.57

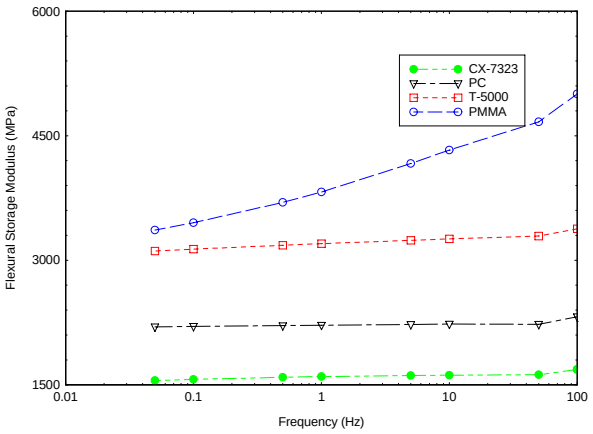

Figure 4. Flexural Storage Modulus as a function of Frequency.

3.5 Compressive Properties

Rate effects on compressive properties of ¼" PC and PMMA are shown in Figure 5 and Table 4. As can be seen, PC is insensitive to all the parameters examined in this study. Figures 5a and c reveal this result by showing no differences in load displacement behavior upon compression rate. However, as shown in the Figures 5b and d, PMMA exhibits catastrophic failure. At slower rates (1mm/min), PMMA shows a clear yield point and breaks catastrophically. At higher rates (50mm/min), the catastrophic failure occurred before the yield point and as the penetration progressed, the remaining portion of the material again failed catastrophically. As a result, the stiffness, which is the slope of the curve, increased and the displacement decreased with increasing compression rate. Hence, the total energy absorbed during the penetration decreased considerably with increasing compression rate. Previous study shows that ballistic energy absorption of PC is significantly greater than PMMA at the thickness range examined in this study (1/4"). However, at higher velocities above the ballistic limit, PMMA exhibits greater energy absorption capability over PC[1].

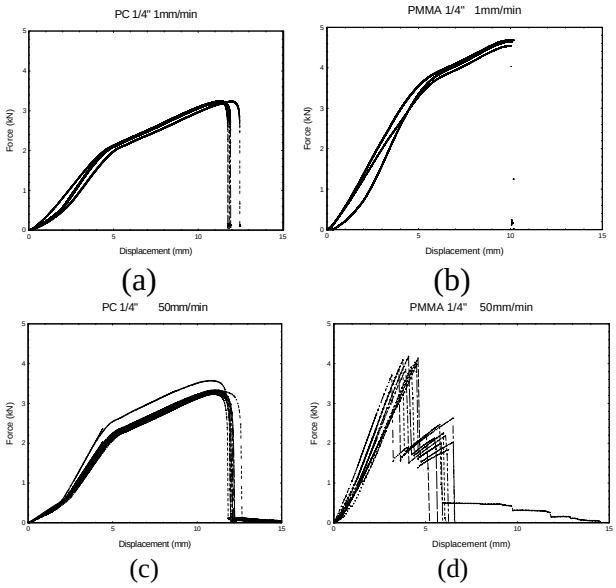

Figure 5. Load Displacement traces under compression of PC and PMMA at 1mm/min (a and c) and 50mm/min (b and d) rate of compression, respectively.

Table 4. Compression property data at various compression rates of PC and PMMA. Xmax is the maximum displacement at a maximum force (Fmax) and Stiffness is the initial slope of the curve.

Rate (mm/min)	Thickness (mm)	Xmax (mm)	Fmax (kN)	Total Energy (J)	Stiffness (N/m)
		PMMA			
1	5.82	9.98	4.64	29.37	0.84
10	5.95	7.93	4.84	21.98	1.06
25	5.96	4.58	3.92	11.35	1.12
50	6.08	4.16	3.97	11.38	1.14
		PC			
1	5.4	11.46	3.23	23.81	0.57
10	5.45	10.46	3.23	21.73	0.60
25	5.43	11.25	3.26	24.72	0.61

Figure 6 and Table 5 show the material behavior under constant compression rate. As could be expected from the compression rate effect, PMMA again exhibited catastrophic failure. The other three materials generally performed similarly.

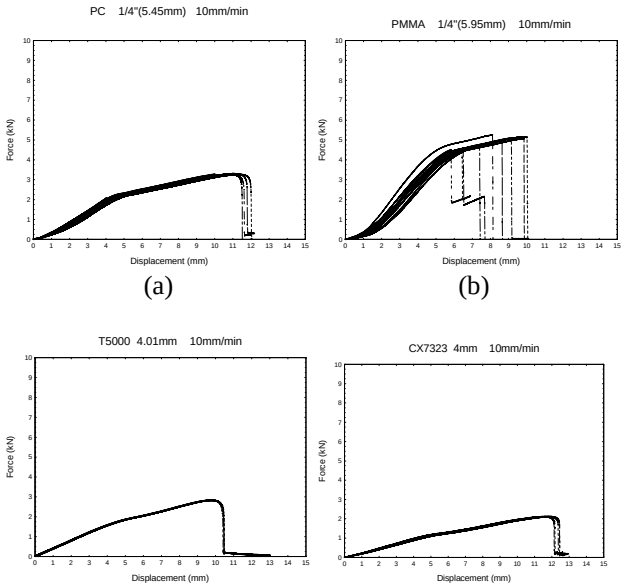

Figure 6. Typical compression behavior of PC (a), PMMA (b), T-5000 (c) and CX-7323 (d) at the compression rate of 10mm/min.

Table 5. Compression properties of the polymers. Xmax is the maximum displacement at a maximum force (Fmax) and Stiffness is the initial slope of the curve.

Materials	Thickness (mm)	Xmax (mm)	Fmax (kN)	Total Energy (J)	Stiffness (kN/mm)
PC	0.73	8.55	0.36	1.08	0.06
	3.04	10.52	1.62	7.68	0.185
	5.45	10.75	3.23	20.08	0.6
PMMA	1.47	7.22	0.69	1.76	0.13
	5.95	7.43	4.85	21.26	1.06
	9.29	6.72	8.82	27.62	2.21
T-5000	1.29	9.05	0.79	2.72	0.13
	2.03	9.76	1.372	5.8	0.178
	3.02	10.49	2.128	10.7	0.245
	4.01	10.46	2.828	16.15	0.406
	10	12.87	8.42	48.99	2.36
CX-7323	1.06	10.09	0.51	1.77	0.082
	2.03	11.46	1.028	4.76	0.132
	2.98	12.08	1.54	8.56	0.162
	4	12.33	2.106	13.81	0.248
	9.96	13.68	5.44	38.88	1.47

In Figure 7, the stiffness of the materials was compared. At relatively thin samples, the stiffness did not change significantly between the materials. However, noticeable deviation of the stiffness started around the 3mm thickness region. As one might expect, it shows a reasonably clear distinction between a group of relatively stiff materials (PMMA and T-5000) and a group of relatively ductile materials (PC and CX-7323).

Total energy absorption during compression failure is shown in Figure 8. Total energy absorption of T-5000, CX-7323 and PC exhibit steady increase with increasing thickness. However, PMMA, which has stiffness comparable to T-5000, showed lower values than T-5000. This is due to the premature failure of PMMA even before the yield point.

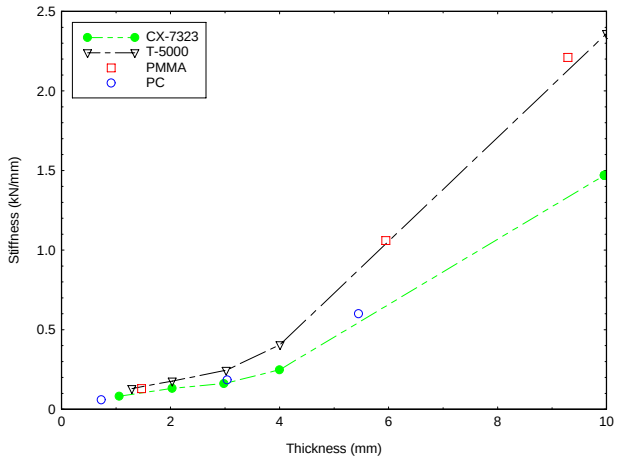

Figure 7. Stiffness as a function of sample thickness.

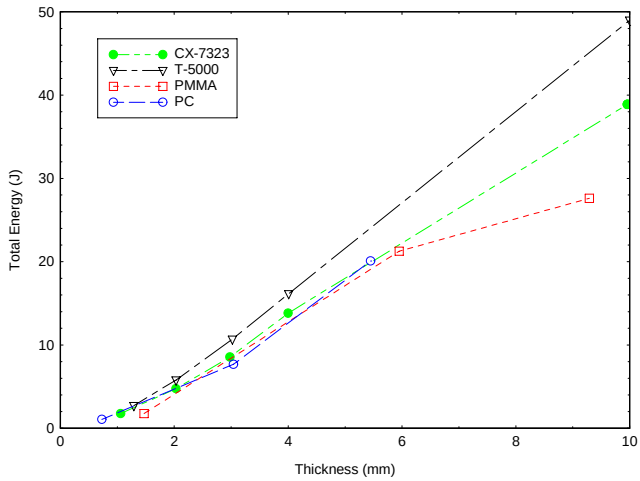

Figure 8. Total energy as a function of sample thickness

3.6 Abrasion Resistance

Figure 9 shows the taber abrasion resistance of PC and CX-7323. Results on both coated and uncoated samples are shown. A proprietary urethane based abrasion resistant as well as anti-fog coating material was applied through a contract agreement with the Paulson

Manufacturing Corporation. As mentioned in previous section, abrasion resistance was determined by the changes in haze before and after exposure to the abraders.

Although the requirement specified in military specification (Mil-C-83409) for the taber resistance is 50cycles with 500g weight, in order to observe the behaviors in a wide range, testing was done up to 1000cycles. Uncoated PC and CX-7323 performed similarly throughout the test range. For uncoated samples, the percent haze values initially increased rapidly and leveled off starting at 100cycles. As shown in Figure 9, coating significantly improves the abrasion resistance for a small number of cycles until around 100cycles. However, percent haze values increased rapidly above 200cycles. Moreover, at above 500cycles, coated samples showed even higher than uncoated samples.

These results suggest that the soft urethane base coating material completely peeled off from the substrate upon excessive abrasion by breaking the interfacial bond between them. The breakage of the interface bonding between the coating material and the substrate probably created a softer surface than the uncoated surface. Detailed analyses of the cause of these behaviors as well as optimization of the hardness of the coating material and coating processing are currently underway. Until about 100cycles of abrasion, both PC and CX-7323 showed identical behavior and the percent haze values at 50cycles for both are within the requirement stated in Mil-C-83409. Also shown in Figure 9 is that the abrasion resistance of coated PC exhibited noticeably worse performance than coated CX-7323 upon excessive abrasion (above 200cycles).

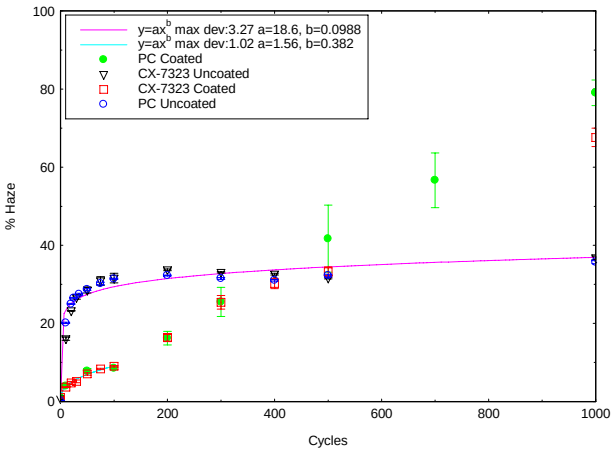

Figure 9. Taber abrasion resistance of abrasion resistance coated as well as uncoated PC and CX-7323.

Figure 10 shows the abrasion resistance against sand blast. Testing was done on CX-7323 and the currently fielded PC goggle. Testing was performed with exposure times up to 60 minutes. For coated CX-7323 samples, the testing was done twice on each sample by doubling the exposure time. As it can be seen in Figure 10, the differences between coated and uncoated samples are significant. Percent haze values of coated samples also showed unacceptable level after 5 minutes of exposure. However, after they were washed with water, the values went down to almost the original state. The PC goggle currently used in the military, however, did not make a significant improvement after washing. The same behavior was observed in uncoated CX-7323 samples. As also shown in Figure 10, the same CX-7323 samples (1st run) were again exposed in the same manner as the first time and the percent haze was measured again (2nd run). As it is shown in Figure 10, the percent haze values of second run samples were slightly increased from the first run. However, the differences are all within the experimental scattering range and their values are still within requirements. These results suggest that the soft urethane coating prevents penetration of the sand particles to the substrate by holding them without permanent adhesion before the particles are washed out.

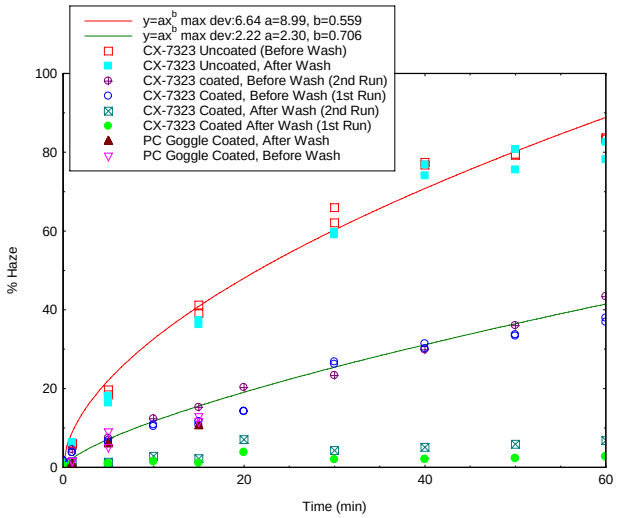

Figure 10. Sand blast abrasion resistance of CX-7323 and currently fielded coated PC goggle.

3.7 Ballistic Evaluation

Figure 11 shows the V_{50} ballistic limit of monolithic TROGAMIDs as well as PC and PMMA. As mentioned earlier, monolithic PMMA outperformed PC at around 3lbs/ft^2 areal density or 10mm thickness. Typical failure modes of these four materials are shown in Figure 12. PMMA shows brittle failure with severe micro cracking around the impact area at high impact velocity or on thick samples. T-5000 also exhibits brittle failure with radial cracking upon penetration. PC and CX-7323, which are relatively softer than PMMA and T-5000, show ductile behavior upon ballistic impact. Although the ballistic failure modes and the mechanical properties

evaluated above clearly differentiate the T-5000 and CX-7323, the overall behavior of these two nylons under ballistic impact is similar (see Figure 11). It seems that the brittle nature of T-5000 was somewhat noticeable in low areal densities by exhibiting lower V_{50} than CX-7323. However, the ballistic impact resistance of T-5000 at very low areal densities was still significantly higher than PMMA.

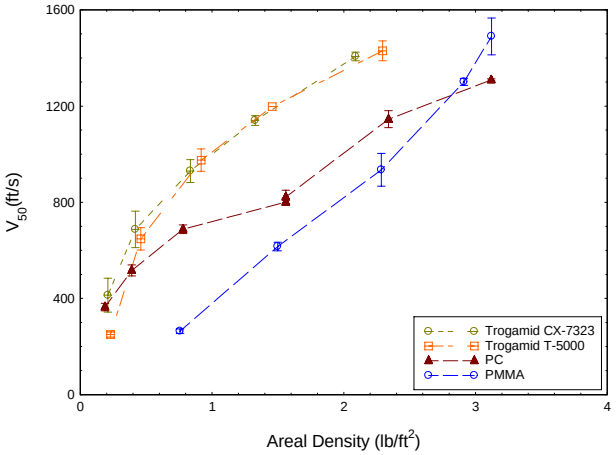

Figure 11. Ballistic limit (V_{50}) as a function of areal density.

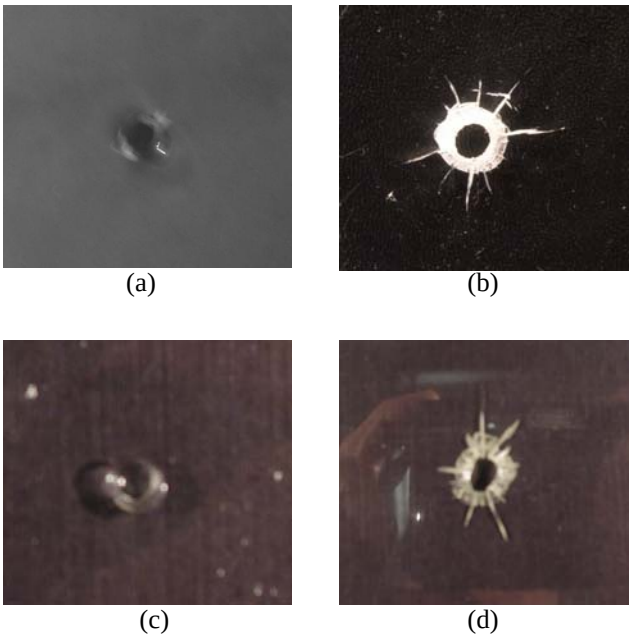

Figure 12. Typical failure modes of PC (a), PMMA (b), CX-7323 (c) and T-5000 (d) under ballistic impact. Projectile used was 17-grain fragment simulating projectile (FSP).

The impact rate effect on the kinetic energy absorption of TROGAMIDs was examined and compared with PC and PMMA. As shown in Figure 13, the energy absorption capability of PMMA increased exponentially with increasing impact rate or striking velocity. However PC as well as the two TROGAMIDs did not show a sensitive response. The most sensitive responses observed in PMMA in the frequency sweep of dynamic mechanical analysis (DMA) and in the rate of compression on the compressive property evaluation described in previous sections are well correlated with the ballistic impact behavior. This unique characteristic of PMMA is most pronounced when it is hybridized [1]. When PMMA is combined with PC, ballistic properties increased drastically and the magnitude of improvement of the hybrid systems is close to the equivalent values of the additive performance of PC and PMMA [1]. Although not as drastic as PMMA/PC hybrids, T-5000/CX-7323 hybrids also show a synergistic effect.

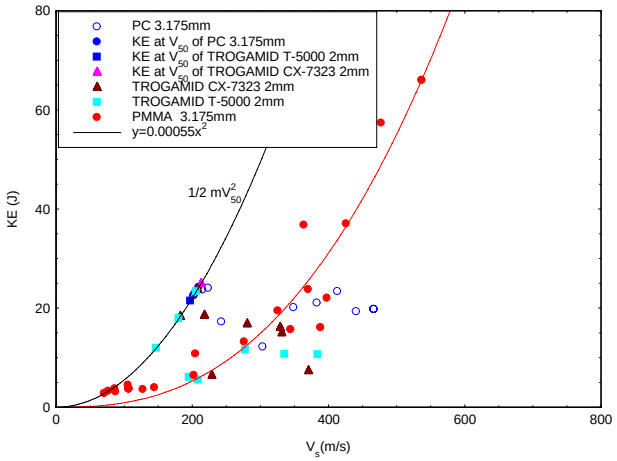

Figure 13. Kinetic energy absorption behavior of the materials as a function of striking velocity on and above V_{50} limits.

Figure 14 shows the comparison of hybrids of T-5000/CX-7323 pair and PMMA/PC pair. The backing material for PMMA/PC hybrids was PC and for T-5000/CX-7323 was CX-7323. These data indicate that, although the differences are small, T-5000/CX-7323 pair exhibited a slight advantage. These results suggest that the further optimization of hybrid systems could be obtained through various brittle/ductile material combinations.

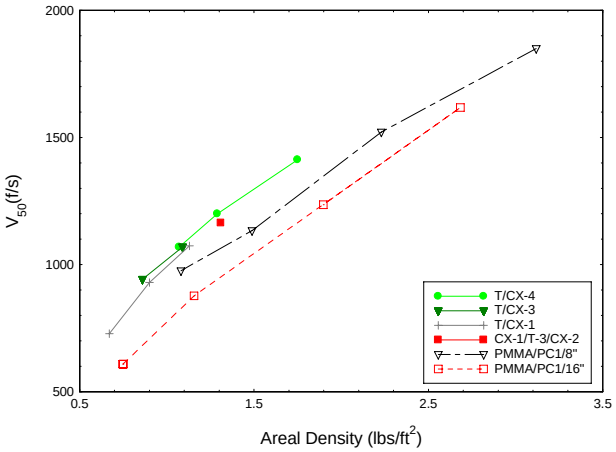

Figure 14. Ballistic limit (V_{50}) data of hybrids.

4. CONCLUSIONS

Ballistic impact resistance as well as relevant mechanical, thermal and optical properties of two new types of nylons were evaluated and compared with PC and PMMA, which are the commonly used materials for current transparent armor applications. Flexural and compressive properties obtained from Instron and DMA clearly grouped the brittle nature of PMMA and T-5000 as one group and the ductile nature of PC and CX-7323 as another. PMMA exhibited the most sensitive response to frequency observed in the DMA analysis as well as on the rate of compression. This behavior is consistent with the sensitive response of PMMA upon higher velocity impact observed in previous studies[1]. Both TROGAMID T-5000 and TROGAMID CX-7323 exhibited insensitive response on the ballistic impact velocity above V_{50}. The urethane based coating material showed excellent sand abrasion resistance. The same coating material also met the taber abrasion resistance requirement specified in military specification. However, upon excessive abrasion, the hazeness increased rapidly. Moreover, at above 500 cycles of abrasion, coated samples showed even higher hazeness (hence lower abrasion resistance) than uncoated samples. Although the characteristics of TROGAMID T-5000 and TROGAMID CX-7323 are different, ballistic impact resistance of these two materials are similar throughout the wide range of thickness or areal densities. Except for very thin samples, both monolithic TROGAMIDs showed significantly higher ballistic limits than monolithic PC or PMMA in the areal density range examined in this study.

Acknowledgements

Authors would like to thank Degussa Corporation who supplied the TROGAMID materials and Paulson Manufacturing Corporation who fabricated the TROGAMID samples.

5. REFERENCES

1. John W. Song and Alex J. Hsieh, "Ballistic Impact Resistance of Monolithic, Hybrid and Nano Composites of PC and PMMA", Proceedings of the American Society for Composites 17th Technical Conference (2002)
2. Alex J. Hsieh, John W. Song, Daniel DeSchepper, Paul Moy and Peter G. Dehmer, "The effect of PMMA on Ballistic Impact Performance of Hybrid Hard/Ductile All-Plastic and Glass Based Composites.", in press, Technical report, ARL (2003)
3. Robert W. Lewis and Gordon R. Parsons, "Ballistic Performance of Transparent Materials for Eye Protection", Technical Report, Army Materials and Mechanics Research Center, AMMRC TR 72-36 (Nov. 1972)
4. Thomas Tassinari, Private Communications.